The glutamic acid-rich–long C-terminal extension of troponin T has a critical role in insect muscle functions

Received for publication, November 21, 2019, and in revised form, February 3, 2020 Published, Papers in Press, February 5, 2020, DOI 10.1074/jbc.RA119.012014

Tianxin Cao, Alyson Sujkowski, Tyler Cobb, Robert J. Wessells, and Jian-Ping Jin[1]

From the Department of Physiology, Wayne State University School of Medicine, Detroit, Michigan 48201

Edited by Enrique M. De La Cruz

The troponin complex regulates the Ca^{2+} activation of myofilaments during striated muscle contraction and relaxation. Troponin genes emerged 500–700 million years ago during early animal evolution. Troponin T (TnT) is the thin-filament–anchoring subunit of troponin. Vertebrate and invertebrate TnTs have conserved core structures, reflecting conserved functions in regulating muscle contraction, and they also contain significantly diverged structures, reflecting muscle type- and species-specific adaptations. TnT in insects contains a highly-diverged structure consisting of a long glutamic acid–rich C-terminal extension of ~70 residues with unknown function. We found here that C-terminally truncated *Drosophila* TnT (TpnT–CD70) retains binding of tropomyosin, troponin I, and troponin C, indicating a preserved core structure of TnT. However, the mutant $TpnT^{CD70}$ gene residing on the X chromosome resulted in lethality in male flies. We demonstrate that this X-linked mutation produces dominant-negative phenotypes, including decreased flying and climbing abilities, in heterozygous female flies. Immunoblot quantification with a TpnT-specific mAb indicated expression of TpnT–CD70 *in vivo* and normal stoichiometry of total TnT in myofilaments of heterozygous female flies. Light and EM examinations revealed primarily normal sarcomere structures in female heterozygous animals, whereas Z-band streaming could be observed in the jump muscle of these flies. Although TpnT–CD70-expressing flies exhibited lower resistance to cardiac stress, their hearts were significantly more tolerant to Ca^{2+} overloading induced by high-frequency electrical pacing. Our findings suggest that the Glu-rich long C-terminal extension of insect TnT functions as a myofilament Ca^{2+} buffer/reservoir and is potentially critical to the high-frequency asynchronous contraction of flight muscles.

Muscle contraction is a vital function of animals. Striated muscles represent a highly-differentiated tissue type characterized by bundles of myofibrils consisting of tandem repeats of sarcomeres that make up the contractile units (1). The sarcomeres are formed by overlapping myosin thick filaments and actin thin filaments. In the vertebrate skeletal and cardiac muscles, contraction is powered by actin-activated myosin ATPase under the regulation of intracellular Ca^{2+} via the troponin complex in the thin filament (1–3). The myofilament protein contents of vertebrate and invertebrate striated muscle sarcomeres are conserved, with both containing the thin-filament regulatory proteins tropomyosin and troponin (4). The troponin complex has three protein subunits as follows: the calcium-binding/receptor subunit troponin C (TnC)[2]; the inhibitory subunit troponin I (TnI); and the tropomyosin-binding/thin-filament–anchoring subunit troponin T (TnT) (3–5).

Troponin emerged during early animal evolution ~700 million years ago. Genes encoding the subunits of troponin are found in all invertebrate animals higher than Cnidaria (jellyfish and sponges) (6). This phylogenetic chronicle corresponds to the emergence of the central nervous system (7), implying an essential role of troponin in the more coordinated muscle contractions of higher animal species. To study the molecular evolution of troponin by characterizing its conservation and diversity in invertebrate and vertebrate muscles is a powerful approach to understand the structure–function relationship of troponin in determining muscle contractility in physiological and pathophysiological conditions.

By interaction with tropomyosin in the thin filament, TnT plays an organizer role in the center of the sarcomeric Ca^{2+}-regulatory system (8). Vertebrates have evolved with three homologous genes encoding the cardiac, fast, and slow skeletal muscle-type isoforms of TnT, whereas most invertebrates such as insects have only a single TnT gene (6). Gene structure and molecular evolution studies identified the fast skeletal muscle TnT as the ancestral form of the three vertebrate muscle-type–specific isoforms (9). The phylogenetic tree in Fig. 1*A*, constructed from protein sequences of representative invertebrate TnT and vertebrate fast TnT, shows their evolutionary lineage and overall divergence.

Previous studies have extensively demonstrated the critical role of troponin in the Ca^{2+} regulation of insect muscle contraction (10). The *Drosophila TpnT* locus on chromosome X encodes several physiological alternative splicing variants, whereas aberrant splicing or missense mutations cause muscle abnormalities such as the upheld and indented thorax pheno-

This work was supported in part by National Institutes of Health Grants HL127691 and HL138007 (to J.-P. J.) and AG059683 (to R. J. W.). The authors declare that they have no conflicts of interest with the contents of this article. The content is solely the responsibility of the authors and does not necessarily represent the official views of the National Institutes of Health.
The nucleotide sequence(s) reported in this paper has been submitted to the GenBank™/EBI Data Bank with accession number(s) MK227440.

[1] To whom correspondence should be addressed: Dept. of Physiology, Wayne State University School of Medicine, 5374 Scott Hall, 540 E. Canfield, Detroit, MI 48201. Tel.: 313-577-1520; Fax: 313-577-5494; E-mail: jjin@med.wayne.edu.

[2] The abbreviations used are: TnC, troponin C; TnT, troponin T; TnI, troponin I; IFM, indirect flight muscle; HRP, horseradish peroxidase; PMSF, phenylmethylsulfonyl fluoride; FA, formaldehyde; RFP, red fluorescence protein; RS, relaxing solution; NGS, normal goat serum.

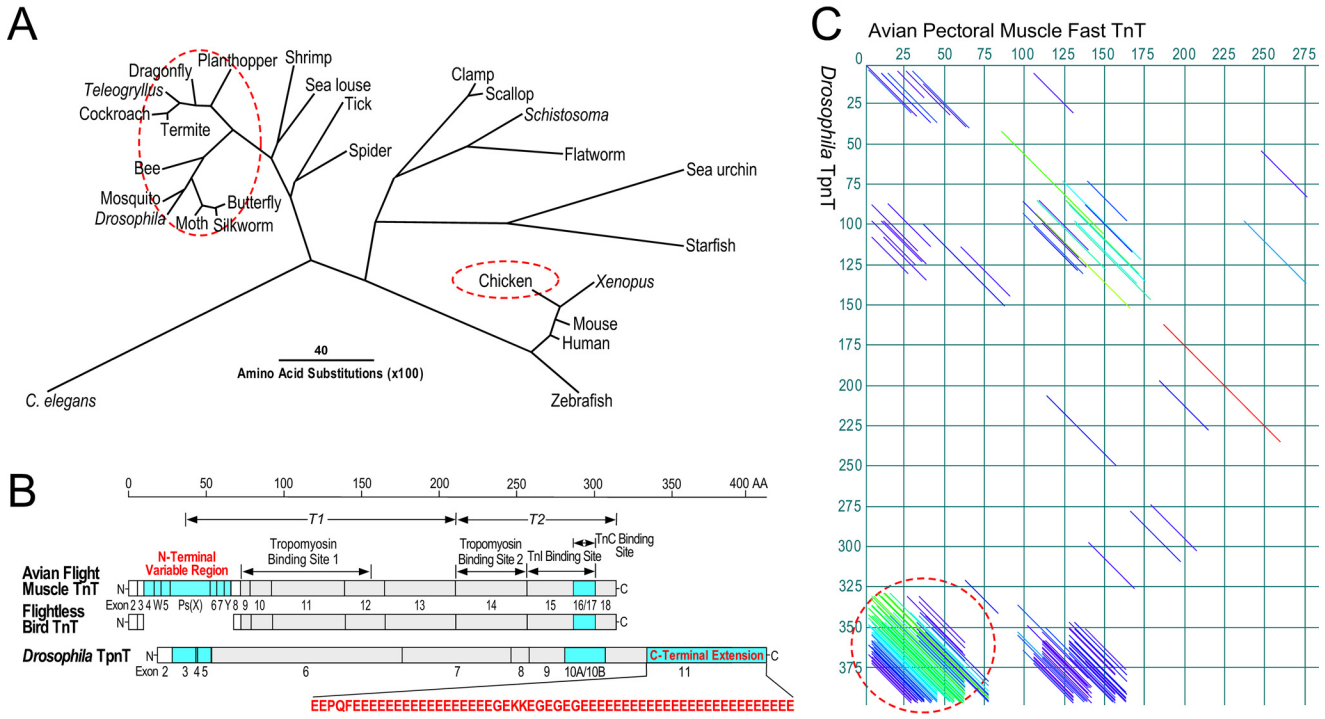

Figure 1. Glu-rich C-terminal extension of insect TnT. *A,* phylogenic tree constructed by aligning amino acid sequences from representative species in various animal phyla using the DNAStar MegAlign Clustal V method illustrates the divergence between vertebrate and insect TnTs. The GenBank™ accession numbers for the sequences compared are as follows: butterfly TnT, BAG30738.1; bee TnT, NP_001035348.1; *C. elegans* TnT, NP_001024704.1; chicken TnT, NP_990253.1; clamp TnT, BAA13610.1; cockroach TnT, AAD33603.1; *Drosophila* TnT, NP_001162742.1; flatworm TnT, XP_024354240.1; frog TnT, NP_989143.1; human TnT, NP_001354775.1; mosquito TnT, XP_001851541.1; moth TnT, ADO33067.1; mouse TnT, NP_001347086.1; planthopper TnT, AGI96988.1; scallop TnT, BAA20456.1; *Schistosoma* TnT, XP_018646291.1; sea louse TnT, ACO12887.1; sea urchin TnT, XP_011671209.1; shrimp TnT, AQV08184.2; silkworm TnT, ABD36267.1; spider TnT, EU247211.1; starfish TnT, XM_022232646.1; *Teleogryllus* TnT, AVI26881.1; termite TnT, AGM32088.1; tick TnT, AAY42205.1; zebrafish TnT, AAF78472.1. *B,* linear maps of protein primary structure outline the region conserved between vertebrate and invertebrate TnTs containing the binding sites for tropomyosin, TnI, and TnC, together with the alternatively spliced N-terminal variable region, a pair of mutually-exclusive alternative coding exons, and the long Glu-rich C-terminal extension unique to insect TnT. In contrast to the long N-terminal variable region in a representative avian flight muscle TnT, the TnT of the flightless bird, emu (accession number XP_025948591.1), represents a vertebrate TnT that has a diminished N-terminal segment. *C,* a dot-plot comparison of amino acid sequences from avian pectoral muscle fast TnT and insect TnT demonstrates the presence of similar Glu-rich segments in the C-terminal extension of *Drosophila* TnT (accession number NP_001162742.1) and the N-terminal variable region of eagle fast skeletal muscle TnT (accession number XP_011597294.1), implicating an analogous role in flight functions.

types (11), muscleblind myotonic dystrophy (12), or abnormal development of flight muscles (13).

Linear structural comparison between vertebrate and *Drosophila* TnT (Fig. 1*B*) shows a large portion of conserved structures corresponding to their conserved core functions. Vertebrate and invertebrate TnTs both have an alternatively-spliced N-terminal variable region (5, 14) and a pair of alternatively-spliced and mutually-exclusive C-terminal coding exons, *i.e.* exons 16 and 17 of vertebrate fast skeletal muscle TnT (15, 16) and exons 10A and 10B of *Drosophila* TnT (13). After several decades of research, the functional significance of these variable structures of TnT remains not fully understood.

A diverged structure of invertebrate TnT found in flying insects is a long C-terminal extension with a high content of glutamic acid residues (Fig. 1*B*) (11). The function of this highly-diverged structure of insect TnT and its fitness value during natural selection are of significant interest. The N-terminal variable region of some vertebrate TnTs also has high Glu contents (5). This similar trait is most striking in the fast skeletal muscle TnT specifically expressed in adult avian pectoral muscles (17). This potentially-convergent structural similarity can be clearly seen in the paired dot-plot comparison between eagle pectoral muscle TnT and *Drosophila* TnT (Fig. 1*C*). Considering that avian leg muscle TnT has a much shorter N-terminal variable region (18) and fast TnT of the emu, a flightless bird, has lost this structure (Fig. 1*B*), we propose that the long Glu-rich segments in insect TnT and avian pectoral muscle TnT may have both evolved from an analogous evolutionary selection for flight abilities.

Supporting this hypothesis, a previous study found that the Glu-rich N-terminal segment of avian pectoral muscle TnT has a physiologically relevant Ca^{2+}-binding capacity (19), which may play a novel role in the Ca^{2+} regulation of muscle contraction. In this study, we genetically engineered flies to demonstrate that deletion of the C-terminal 70 amino acids of *Drosophila* TnT (TpnT–CD70) significantly decreases muscle and heart functions, establishing the biological importance of the Glu-rich C-terminal extension of insect TnT. In the meantime, fly hearts expressing TpnT–CD70 exhibited significantly increased tolerance to Ca^{2+} overloading during high-frequency electrical pacing, supporting the potential role of the Glu-rich segment in TnT as a myofilament Ca^{2+} buffer/reservoir.

Results

Cloned cDNAs encoding two predominantly-expressed and one novel RNA-splicing variants of Drosophila TpnT

cDNAs encoding three N-terminal alternative splicing variants of *Drosophila TpnT* were cloned via RT-PCR from total

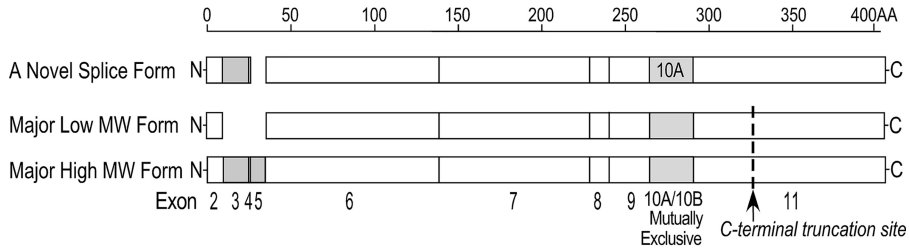

Figure 2. Splicing variants of *Drosophila* TnT cloned in this study. In addition to cDNAs encoding the predominantly-expressed high- and low-molecular-weight (*MW*) N-terminal splice forms, including or excluding the segment encoded by exons 3–5, a cDNA encoding a novel alternative splicing variant excluding exon 5 and containing exon 10A has been cloned. The CD70 truncation site engineered to delete the insect-specific Glu-rich C-terminal extension in the two major splice forms is indicated.

RNA extracted from whole adult flies. The corresponding protein variants are compared in the linear structural maps in Fig. 2. A novel splice form of *Drosophila* TnT with the exon 5-encoded segment in the N-terminal variable region excluded and exon 10A in the C-terminal mutually-exclusive splicing region was identified among the cloned cDNAs. The sequence has been deposited to GenBank™ with accession number MK227440. The other two cDNA variants cloned encode the high- and low-molecular-weight TnT splice forms that are predominantly expressed in normal adult *Drosophila* muscles (Fig. 2).

Production of C-terminal truncated Drosophila TnT in Escherichia coli

Intact *Drosophila* TnT proteins exhibited significant toxicity to host *E. coli* cells and did not yield a preparative level of expression (data not shown). In sharp contrast, *Drosophila* TpnT–CD70 exon 10A and TpnT–CD70 exon 10B proteins with the C-terminal Glu-rich segment removed express in *E. coli* at high levels (Fig. 3). Both exon 10A and exon 10B variants of TpnT–CD70 proteins were purified using conventional biochemical methods (Fig. 3) for functional characterization.

C-terminal truncated Drosophila TnT retains the ability to bind tropomyosin, TnI, and TnC

Because the C-terminal Glu-rich extension is an evolutionarily-diverged structure in invertebrates such as insects, we anticipated its deletion would not destroy the core functions of *Drosophila* TnT. To validate this hypothesis, protein-binding studies showed that both exon 10A and exon 10B variants of *Drosophila* TpnT–CD70 have high-affinity binding to rabbit α-tropomyosin (Fig. 4*A*), bovine cardiac TnI (Fig. 4*B*), and chicken fast skeletal muscle TnC in the presence of 0.1 mM $CaCl_2$ (Fig. 4*C*) or 0.1 mM EGTA (Fig. 4*D*), comparable with the control of chicken fast skeletal muscle TnT that is a native binding partner of the vertebrate tropomyosin, TnI, and TnC used in this study to overcome the lack of purified insect myofilament proteins. The biochemical assessment demonstrates that deletion of the C-terminal Glu-rich segment does not abolish the core functions of *Drosophila* TnT.

Within the physiological range, *Drosophila* TpnT–CD70 proteins showed lower affinity for vertebrate tropomyosin but higher affinity for vertebrate TnI (Fig. 4, *A* and *B*). The binding of TpnT–CD70 proteins to TnC is Ca^{2+}-dependent, similar to that of chicken fast TnT (Fig. 4*D*) and consistent with previous studies of vertebrate troponin (20). The preserved biochemical

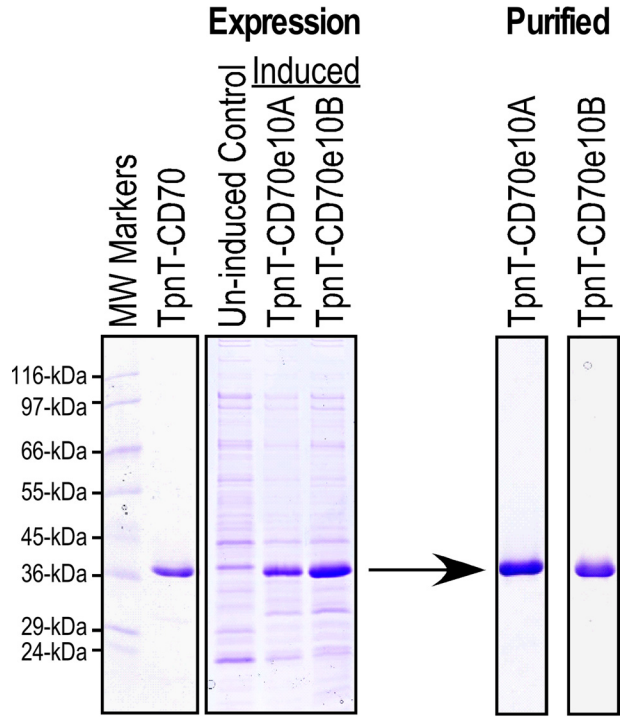

Figure 3. Expression and purification of *Drosophila* TpnT–CD70 proteins. 14% SDS-polyacrylamide gels demonstrate examples of the high-level expression of TpnT–CD70 exon 10A and TpnT–CD70 exon 10B proteins in *E. coli* culture and the purified proteins.

activities of TnT–CD70 proteins indicate their preserved core functions in muscle thin-filament regulation.

The presence of the mutually-exclusive alternative exons 10A or 10B produced different binding affinities for tropomyosin and TnC (Fig. 4), indicating functional impacts of this alternatively-spliced segment of TnT, which are under investigation together with the vertebrate counterparts, exon 16 and exon 17, in fast TnT (5, 6).

TpnT–CD70 mutant flies

With the evidence that deletion of the C-terminal Glu-rich segment does not abolish the core function in *Drosophila* TpnT–CD70 protein (Fig. 4), *TpnT–CD70* mutant flies were developed. Illustrated in Fig. 5, the mutant allele was constructed by inserting a stop codon in exon 11 of the *TpnT* gene on chromosome X using CRISPR/Cas9 genomic editing to truncate the last 70 amino acids of the polypeptide chain and delete the C-terminal Glu-rich segment. The red fluorescence protein (RFP) selection marker was subsequently removed by

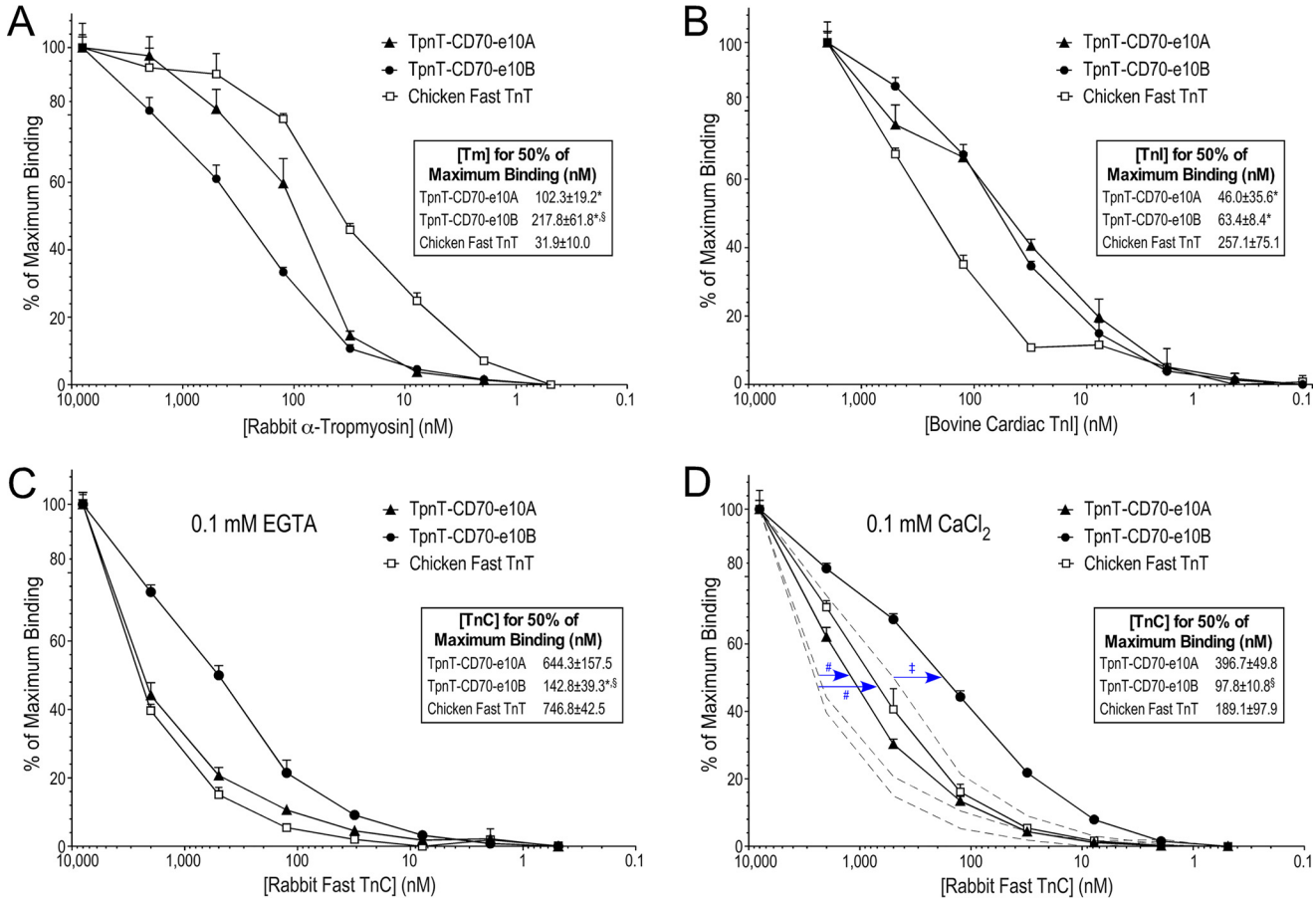

Figure 4. C-terminal extension-deleted *Drosophila* TnT retains the binding affinity for tropomyosin, TnI, and TnC. The ELISA protein binding curves normalized to maximum binding showed high-affinity binding of *Drosophila* TpnT–CD70 exon 10A and *Drosophila* TpnT–CD70 exon 10B for rabbit α-tropomyosin (*A*), bovine cardiac TnI (*B*), chicken fast skeletal muscle TnC in 0.1 mM EGTA (*C*), or 0.1 mM $CaCl_2$ (*D*). Chicken fast skeletal muscle TnT, a native partner of vertebrate tropomyosin, TnI ,and TnC used in the assays, was employed as control. The *insets* present the protein concentrations required for 50% maximum binding. Although the *Drosophila* TpnT–CD70 exon 10A and 10B variants exhibited lower or higher binding than that of the native control, chicken fast TnT, the affinities are all in the physiological range, demonstrating their preservation of TnT core structure and function. Consistently, the binding of *Drosophila* TpnT–CD70 proteins to TnC remains Ca^{2+}-dependent (the Ca^{2+}-dependent increases in affinity from that in EGTA shown as decreases in TnC concentration required for 50% maximum binding are indicated by the *arrows* in *D*). *Drosophila* TpnT–CD70 exon 10A and 10B variants showed different binding affinities for tropomyosin and TnC. *, $p < 0.05$ *versus* chicken fast TnT; §, $p < 0.05$ *versus* TpnT–CD70 exon 10A; ‡, $p < 0.05$ *versus* EGTA, all in two-tail Student's *t* test; and #, $p < 0.05$ *versus* EGTA in one-tail Student's *t* test.

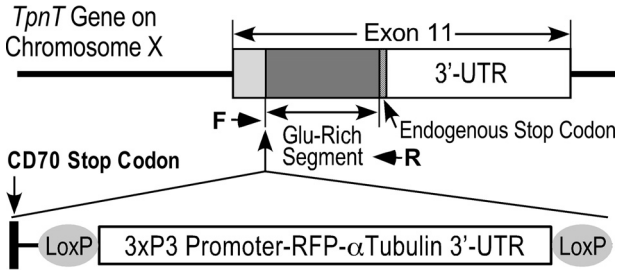

Figure 5. Targeted mutagenesis in *Drosophila TpnT* gene using CRISPR/Cas9 genomic editing. The strategy used to insert a stop codon in exon 11 of the *Drosophila TpnT* gene, which truncates the encoded TnT protein to delete the C-terminal 70 amino acids, is shown. The RFP cassette inserted for the initial selection was excised by Cre-loxP recombination before phenotype studies. Positions of the forward (*F*) and reverse (*R*) primers used in PCR genotyping are indicated on the construct map, which amplify a 221-bp product from wildtype *TpnT* allele and a 297-bp product from the *TpnT–CD70* mutant allele after Cre-loxP–mediated deletion of the RFP cassette.

crossing with a Cre line to establish a line of RFP^- $TpnT^{CD70}$ mutant fly. After confirmation by DNA sequencing of the targeted region, phenotypic studies were performed using both RFP^+ and RFP^- mutant flies.

Although the CD70 truncation of *Drosophila* TnT does not abolish its biochemical functions (Fig. 4), the $TpnT^{CD70}$ allele produced embryonic lethality *in vivo*. Shown in the segregation pattern during breeding (Table 1), the X-linked $TpnT^{CD70}$ mutation causes 100% death of mutant males before hatching. Therefore, $TpnT^{CD70}$ homozygous females would be lethal as well, although test breeding could not be done due to the lack of mutant male parents.

With the presence of one WT X chromosome, heterozygous $TpnT^{CD70/+}$ females are viable and fertile, appearing in the expected Mendelian ratio (Table 1). Therefore, $TpnT^{CD70/+}$ females were used as subjects for phenotypic characterization.

High-affinity mAb specifically recognizes all alternative splice forms of Drosophila TnT and the CD70 truncation

From immunization using *Drosophila* TpnT–CD70 protein, a mouse hybridoma cell line secreting anti-*Drosophila* TnT mAb (2C12) was established after multiple rounds of subcloning. Characterization of the hybridoma cell culture supernatant using Western blotting showed that mAb 2C12 specifically recognizes TnT bands in total muscle homogenates of adult fly and

Table 1

Non-Mendelian segregation of the X-linked *TpnT-CD70* allele demonstrates embryonic lethality

Whereas background control flies emerge in normal Mendelian ratios, $TpnT^{CD70/FM7a}$ flies exhibited non-Mendelian segregation during breeding, demonstrating homozygous lethality of the *TpnT–CD70* allele. Presence of a wildtype copy of *TpnT* is required for survival, as demonstrated by the absence of any viable male or female homozygous $Tpnt^{CD70-/-}$ flies from breeding between $TpnT^{CD70/+}$ heterozygote female and wildtype male, corresponding to ~25% loss of embryos due to the X-linked $TpnT^{CD70}$ mutation. NA, not applicable.

Parents	Embryos	Hatching rate	WT♀	$TnT^{CD70/+}$♀	WT♂	TnT^{CD70}♂	WT♀/total embryos	WT♂/total embryos	$TnT^{CD70/+}$♀/total embryos	TnT^{CD70}♂
WT♀×WT♂	660	98.0%	311	NA	336	NA	48.1%	51.9%	NA	NA
$TnT^{CD70/+}$♀×WT♂	607	74.6%	153	150	150	0	25.2%	24.7%	24.7%	0.0%

total protein extracts of whole larvae without detectable cross-reaction to any other proteins (Fig. 6*A*). Western blotting showed that mAb 2C12 does not cross-react with cardiac or skeletal muscle TnT in multiple vertebrate species, including the ancestral species hagfish (Fig. 6*A*), indicating its recognition of a fly TnT-specific epitope.

Shown in the high-sensitivity ELISA titration of 2C12 hybridoma culture supernatants in Fig. 6*B*, mAb 2C12 has equally high affinities against the exon 10A and exon 10B variants of *Drosophila* TpnT–CD70 with no cross-reaction to chicken breast muscle fast TnT and human cardiac TnT, confirming its specificity to fly TnT under nondenaturing conditions. This new mAb provides a critical tool to examine the expression of TpnT–CD70 proteins in mutant fly muscle and heart and to establish the causal effect on functional phenotypes.

The Western blotting data in Fig. 6*A* further show that there are two major TnT splice forms expressed in adult *Drosophila* muscles, of which the low-molecular-weight form is predominant in the indirect flight muscle (IFM), whereas the adult jump muscles express both splice forms at similar levels. In contrast, the total protein extracts from *Drosophila* larvae predominantly express the high-molecular-weight splice form (Fig. 6*A*).

With protein controls expressed in *E. coli* from cloned cDNAs (Fig. 7), the high- and low-molecular-weight splice forms of TnT predominantly expressed in adult *Drosophila* muscles correspond to the two previously identified N-terminal alternative splicing variants shown in Fig. 2. An intermediate size TnT splice form was detected in *Drosophila* larva (Fig. 6*A*), of which the exon inclusion pattern and developmental and functional significance remain to be investigated.

Expression and myofilament integration of TpnT–CD70 protein in mutant fly muscles

Age-matched (5 and 14 days old as noted for each experiment) female $TpnT^{CD70/+}$ heterozygote and w^{1118} control flies were studied for muscle and heart phenotypes. We first examined the expression of the TpnT–CD70 protein in mutant fly muscles *in vivo* to validate this new experimental model. mAb 2C12 Western blottings on total protein extracted from flight and jump muscles isolated from $TpnT^{CD70/+}$ heterozygote female flies detected significant amounts of two variants of truncated TnT proteins (Fig. 7). To confirm them as the C-terminal truncated version of the two N-terminal alternative splice forms (Fig. 2) that are predominantly expressed in adult fly muscles (Fig. 6*A*), we showed their SDS gel mobility identical to that of the corresponding CD-70 protein size controls expressed in *E. coli* from cloned cDNA (Fig. 7).

The levels of TpnT–CD70 proteins relative to their intact counterparts in $TpnT^{CD70/+}$ heterozygote female fly muscles were calculated from Western blotting densitometry (Fig. 7). Removal of the RFP cassette significantly increased the expression of TpnT–CD70 protein in both in IFM and jump muscle (Fig. 7), indicating a negative effect of the RFP cassette on gene transcription and/or mRNA stability.

The ratios of high- and low-molecular-weight splice forms in jump muscles were similar for the intact and CD70 forms (Fig. 7*B*), indicating that the insertion of stop codon in exon 11 did not affect the alternative splicing pattern of the N-terminal coding exons (Fig. 2).

Densitometry quantification of total TnT detected in Western blottings *versus* the level of actin determined in parallel SDS gels showed similar stoichiometry in WT and transgenic fly muscles (Fig. 7), excluding haploid insufficiency from possibly causing the lethality of $TpnT^{CD70}$ male embryos or the phenotypes of heterozygote females.

Previous studies have determined that the level of troponin protein detected in striated muscle cells reflects the actual amount integrated in the myofilaments (21) and nonmyofilament-integrated TnT is rapidly degraded in muscle cells (22). Therefore, the protein stoichiometry study demonstrated that TpnT–CD70 is effectively integrated into the myofilaments in *Drosophila* muscle *in vivo*.

The *in vivo* protein expression and stoichiometry data established that dominant-negative effects of the C-terminal truncation of *Drosophila* TnT causes embryonic lethality in males and the phenotypes of heterozygote females, justifying the *TpnT–CD70* fly model for use as an informative system to investigate the functional significance of the Glu-rich long C-terminal extension of insect TnT.

Decreased muscle functions in $TpnT^{CD70/+}$ flies

To investigate the functional effect of deleting the insect-specific C-terminal Glu-rich extension of TnT on muscle functions *in vivo*, acute flight ability was assessed in heterozygote mutant ($TpnT^{CD70/+}$, without RFP) and WT (w^{1118}) flies. The results in Fig. 8*A* show that the average landing height of the mutant flies was decreased, indicating a negative impact of TnT–CD70 on the function of flight muscles.

Climbing velocity of the mutant flies is also significantly decreased compared with WT control (Fig. 8*B*), consistent with decreased muscle functions. Reduced function is also apparent when endurance is tested by repetitive induction of climbing (Fig. 8*C*), indicating dysfunction in both acute and chronic muscle activities.

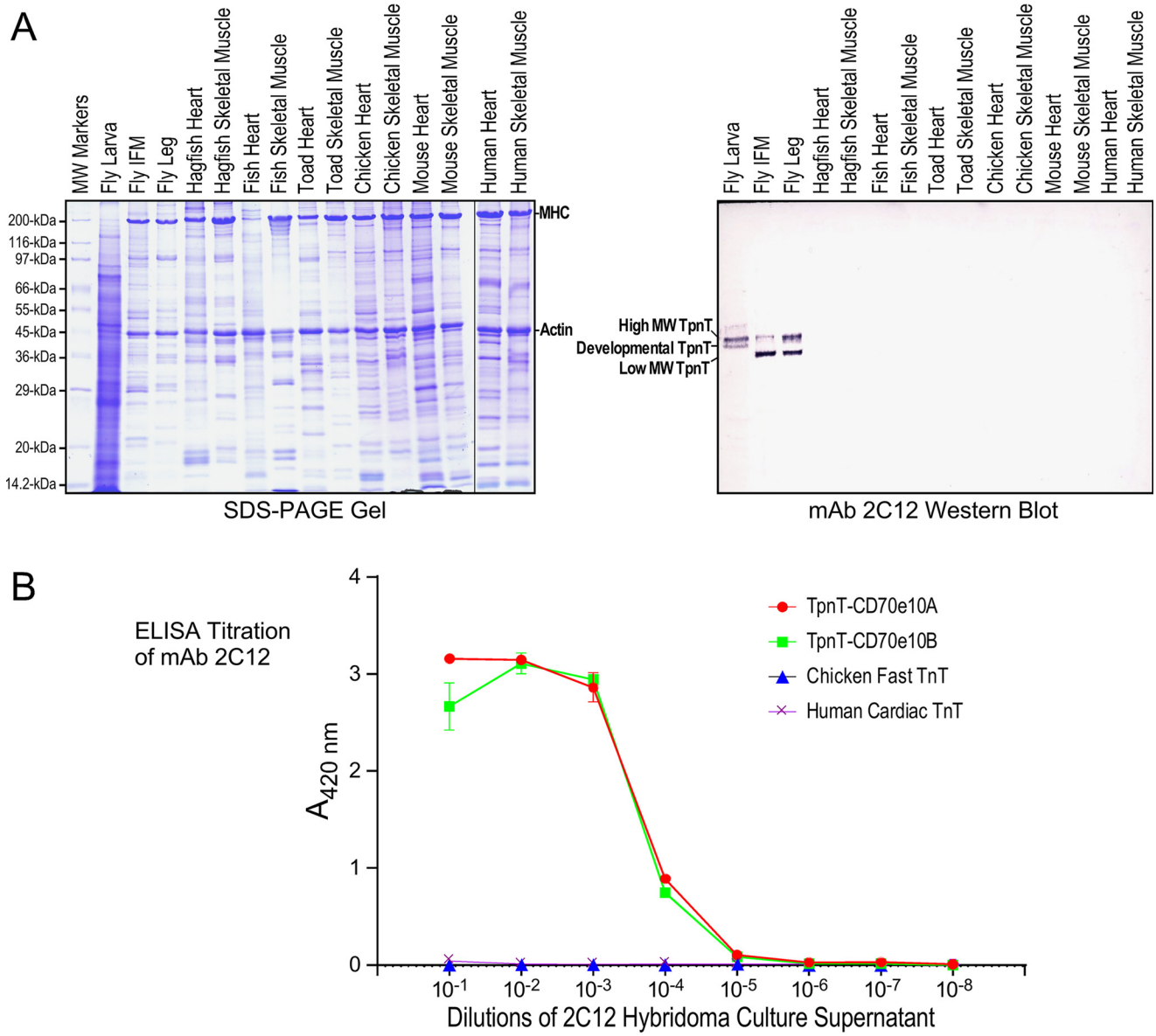

Figure 6. High-affinity mAb 2C12 specifically against *Drosophila* TnT. *A,* specificity of mAb 2C12 was examined using Western blotting on total protein extracts from *Drosophila* larvae and isolated adult muscles together with total protein extracts of cardiac and skeletal muscles from hagfish, bony fish, toad, chicken, mouse, and human. The results showed that mAb 2C12 is highly specific to *Drosophila* TnT with no detectable cross-reaction to any other fly and vertebrate muscle proteins. Three alternative splice forms of *Drosophila* TnT are detected by mAb 2C12, indicating its epitope location in a conserved region. Besides the high- and low-molecular-weight (*MW*) variants found in adult muscles, the developmental variant of *Drosophila* TnT with intermediate size detected in the larval state represents a different splice variant. *MHC*, myosin heavy chain. *B,* ELISA titration of 2C12 hybridoma culture supernatant showed nearly identical high affinities of mAb 2C12 for *Drosophila* TpnT–CD70 exon 10A and exon 10B variants as reflected by the high dilutions for 50% maximum binding. No cross-reaction was detectable to chicken breast muscle TnT and human cardiac TnT in the high-sensitivity ELISA.

Decreased cardiac function in TpnT$^{CD70/+}$ flies

Assessed for functional capacity by pacing at 6 Hz for 30 s, the hearts of *TpnT*$^{CD70/+}$ mutant flies were significantly more sensitive to the stress pacing compared with WT control (Fig. 9*A*), demonstrating that the C-terminal Glu-rich extension of TnT is required for normal cardiac functional durability.

Increased tolerance of TpnT$^{CD70/+}$ fly hearts to short-duration high frequency pacing

To test the hypothesis that the Glu-rich C-terminal extension of insect TnT functions as a myofilament Ca^{2+} buffer/reservoir, as suggested previously for the N-terminal Glu-rich segment of avian pectoral muscle TnT (19), mutant flies were tested in short durations of high frequency cardiac pacing. In contrast to the decreased tolerance to overall cardiac stress shown in Fig. 9*A*, *TpnT*$^{CD70/+}$ hearts were more resistant to 5-s episodes of high frequency pacing, with fewer fibrillation (Fig. 9*B*) and arrest (Fig. 9*C*) events than WT control. This result suggests that the mutant fly hearts are more resistant to acute Ca^{2+} overloading produced by the electrical pacing–induced membrane depolarization of cardiomyocytes. This novel finding supports the notion that removal of the long Glu-rich C-terminal extension of *Drosophila* TnT diminishes a Ca^{2+} buffer in the myofilaments, resulting in a lower baseline content of Ca^{2+}, which allows cardiomyocytes to better tolerate acute Ca^{2+} overloading.

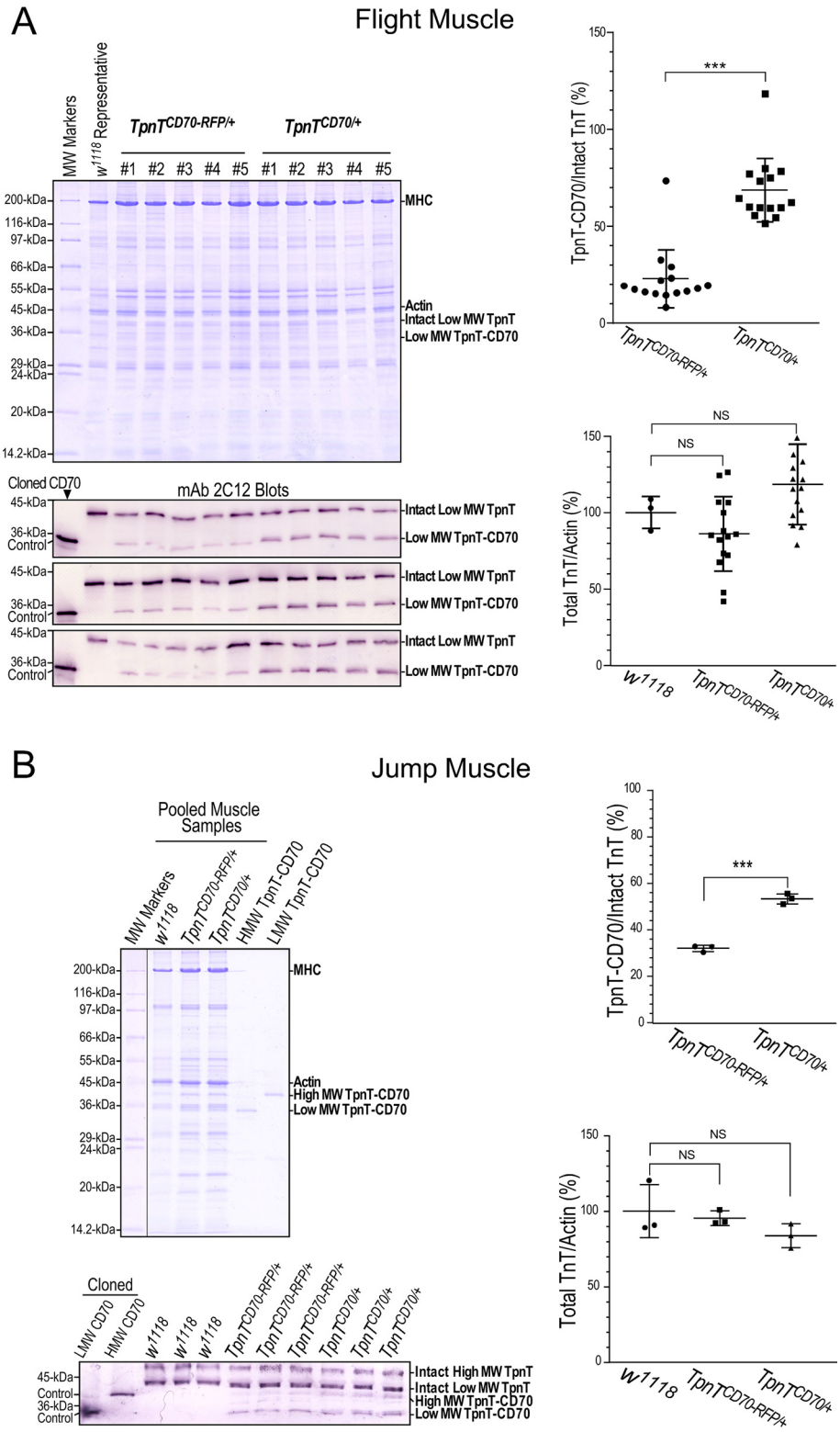

Figure 7. Expression and myofilament integration of TpnT–CD70 protein in *Drosophila* muscles. *A,* SDS-polyacrylamide gel and Western blots of the IFM of genotype-confirmed individual $TpnT^{CD70/+}$ heterozygous female flies showed the expression of TpnT–CD70 protein identified with the cloned protein control for the natively predominant N-terminal alternative splice form. The expression level is significantly higher after removal of the RFP cassette from 0.22 to 0.68 at the level of endogenous alleles shown in the *upper panel* of densitometry analysis, $n = 15$ in each group. The *lower panel* densitometry analysis of total TnT detected in the Western blottings *versus* the level of actin determined in parallel SDS gels showed similar stoichiometry in the muscles of WT and *TpnT–CD70* flies ($n = 3$–15), precluding haploid deficiency. *B,* SDS gel and Western blot densitometry analysis of pooled jump muscles of w^{1118} and *TpnT–CD70* flies further showed that the two predominant splice forms of TpnT–CD70 protein (Fig. 2) identified with cloned protein controls are expressed in the jump muscle of $TpnT^{CD70/+}$ heterozygous female flies at levels lower than that in the IFM of the same flies with ratios to intact endogenous counterparts at 0.32 and 0.52 in the presence or absence of the RFP cassette (the *upper panel* of densitometry analysis), whereas the absence of haploid insufficiency was confirmed (the *lower panel* densitometry analysis) ($n = 3$ in each group). ***, $p < 0.001$, *NS*, not significant, $p > 0.05$.

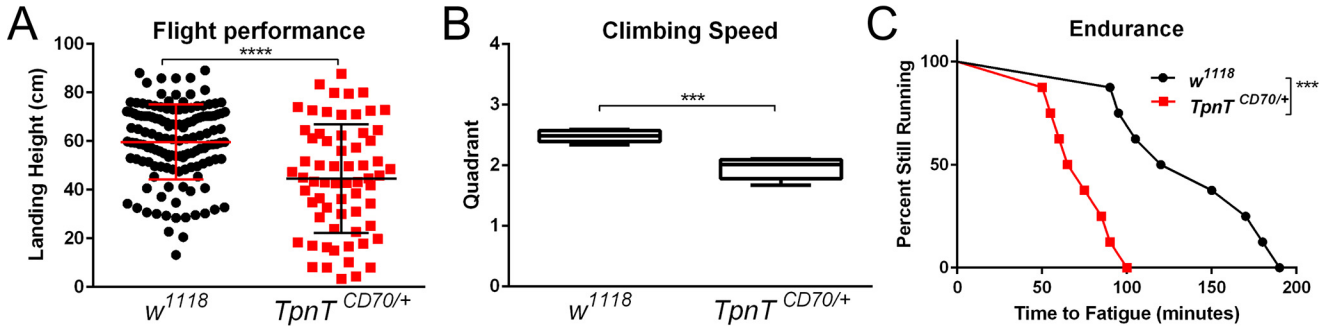

Figure 8. $TpnT^{CD70/+}$ flies have decreased muscle functions *in vivo*. *A*, $TpnT^{CD70/+}$ flies have reduced acute flight performance compared with w^{1118} flies (****, $p < 0.0001$; $n = 160$ per group). *B*, $TpnT^{CD70/+}$ flies have slower climbing speed than w^{1118} control flies (***, $p < 0.0005$; $n = 100$ per group). *C*, $TpnT^{CD70/+}$ flies have lower endurance than controls ($p < 0.0005$; $n = 160$ per group).

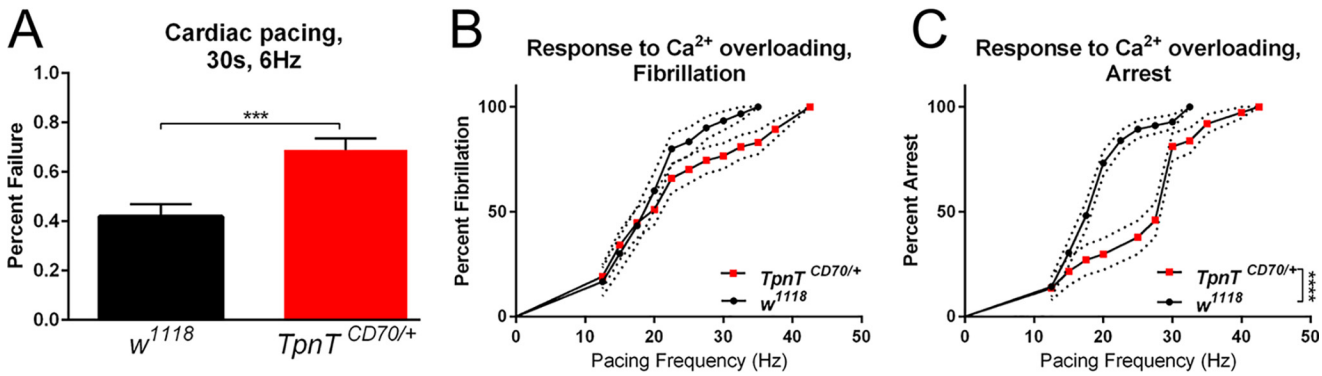

Figure 9. Cardiac pacing studies. *A*, $TpnT^{CD70/+}$ flies showed lower resistance to cardiac stress-pacing at 6 Hz for 30 s than the control of w^{1118} flies (***, $p = 0.001$ in χ^2 test; $n = 100$ per group). *B*, when paced for 5 s with 5-s intervals at progressively increasing frequency to test the effects of Ca^{2+} overloading, $TpnT^{CD70/+}$ fly hearts trend toward a lower fibrillation rate at higher frequencies compared with w^{1118} controls ($p = 0.0868$ in log-rank test, $n \geq 30$). *C*, when scored for cardiac arrest, $TpnT^{CD70/+}$ flies exhibited significantly greater tolerance to high-frequency pacing-induced Ca^{2+} overloading than age-matched w^{1118} controls (****, $p < 0.0001$ in log-rank test, $n \geq 43$). The experiments were performed in duplicate.

Preserved myofibril and sarcomere structure in $TpnT^{CD70/+}$ flies

Whole-mount imaging of heart and muscle tissues of age-matched $TpnT^{CD70/+}$ and control flies showed similar striation patterns without notable overall or regional myofibril disorganization (Fig. 10*A*). Quantitative analysis showed that the resting sarcomeres are longer in the heart (Fig. 10*B*) and jump muscle (Fig. 10*C*) of $TpnT^{CD70/+}$ flies than that in the controls. In contrast, it is not different in IFMs of $TpnT^{CD70/+}$ and control flies (Fig. 10*D*), indicating a likely phenotypic difference between synchronous and asynchronous muscles.

The ultrastructure of $TpnT^{CD70/+}$ mutant fly muscles was examined using transmission electron microscopy (EM) at 14 days of age. Compared with w^{1118} controls, primarily normal sarcomeric structures are seen in both IFM and jump muscle (Fig. 11). $TpnT^{CD70/+}$ jump muscle but not IFM showed signs of Z-band streaming (Fig. 11), which is evidence of the negative impact of deleting the long Glu-rich C-terminal extension of TnT.

Discussion

By interactions with TnC, TnI, and tropomyosin, TnT sits at a central position in the thin-filament regulatory system of striated muscles. It has been extensively studied as an indicator to understand the evolution of vertebrate muscle types. The structural divergence among TnT isoforms and during evolution provides valuable information to understand the structure–function relationship of troponin.

TnT is encoded by a single gene in insects (6). A significantly diverged structure of insect TnT is the Glu-rich–long C-terminal extension (11). Intrigued by the presence of a similarly Glu-rich segment in the N-terminal hypervariable region of vertebrate TnT (Fig. 1), especially the fast TnT in adult avian pectoral muscles (18), we tested the hypothesis that such Glu-rich segments in TnT may have an analogous function that has been convergently selected during the evolution of flight muscles.

Our study found that deletion of the Glu-rich C-terminal extension of *Drosophila* TnT results in dominantly-negative phenotypes in muscle and heart. In the meantime, $TpnT^{CD70/+}$ fly hearts exhibited significantly increased tolerance to Ca^{2+} overloading, supporting a novel role of the Glu-rich segment in TnT as a myofilament Ca^{2+} buffer/reservoir. The following findings provide new insights into key aspects of troponin function in striated muscle myofilament regulation.

Removal of the C-terminal Glu-rich segment from Drosophila TnT does not abolish core biochemical activities

Previous studies in vertebrates have located two tropomyosin-binding sites of TnT: one is in the middle conserved region, and the other is in the beginning of the C-terminal T2 region where the TnI- and TnC-binding sites are also located (Fig. 1*B*) (23). Amino acid sequence alignment showed that the regions containing binding sites for tropomyosin, TnI, and TnC are conserved between vertebrates and *Drosophila* TnTs (Fig. 1, *B* and *C*). *Drosophila* TnT lacking the C-terminal 70 amino acids

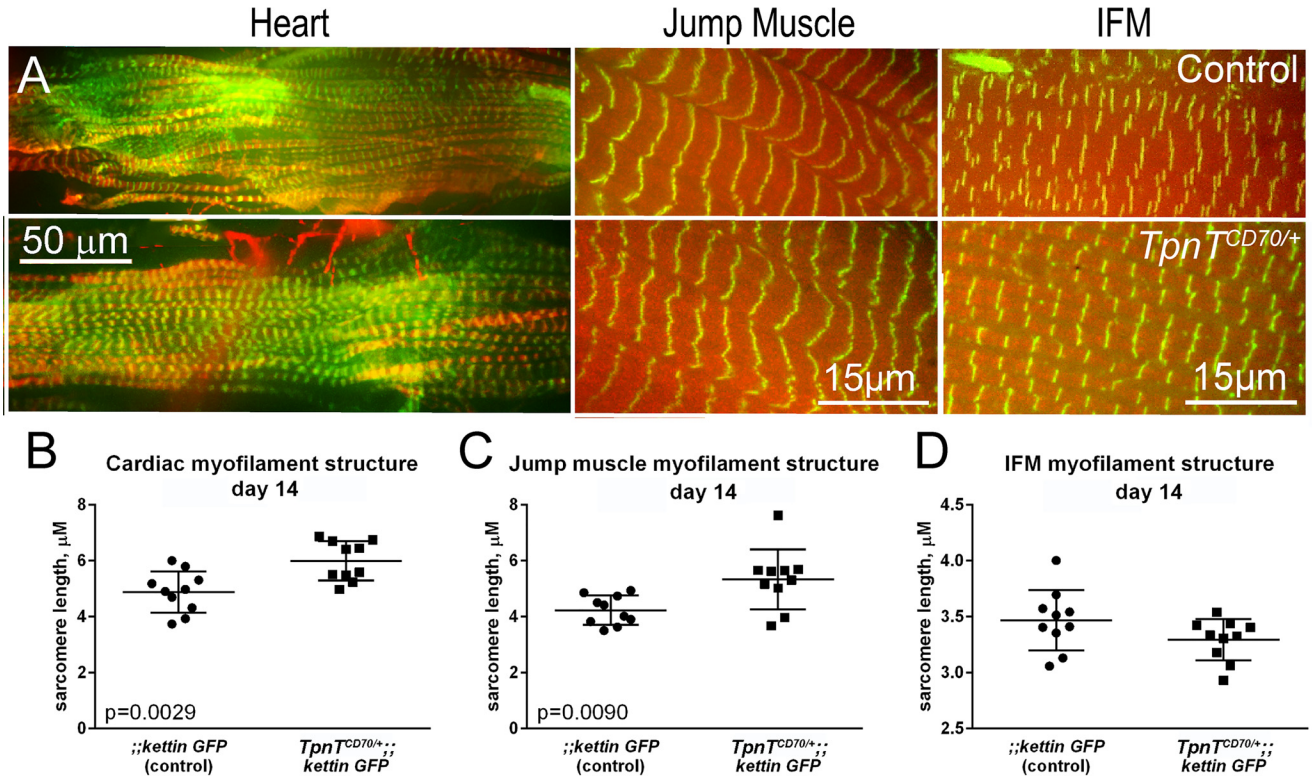

Figure 10. Myofibril and sarcomere structures of $TpnT^{CD70/+}$ mutant flies. *A*, representative whole-mount fluorescence images of heart, jump muscle, and IFM tissues from control (*upper panels*) and $TpnT^{CD70/+}$ (*lower panels*) with *kettin::GFP* to indicate sarcomere Z-discs (*green*) and Alexa fluor 594-phalloidin for F-actin (*red*) show similar striation patterns without myofibril disorganization. Quantitative analysis showed that the resting sarcomeres are longer in the heart (*B*) and jump muscle (*C*) of $TpnT^{CD70/+}$ flies but are not different in IFM (*D*) from age-matched controls, likely reflecting a phenotypic difference between synchronous and asynchronous muscles.

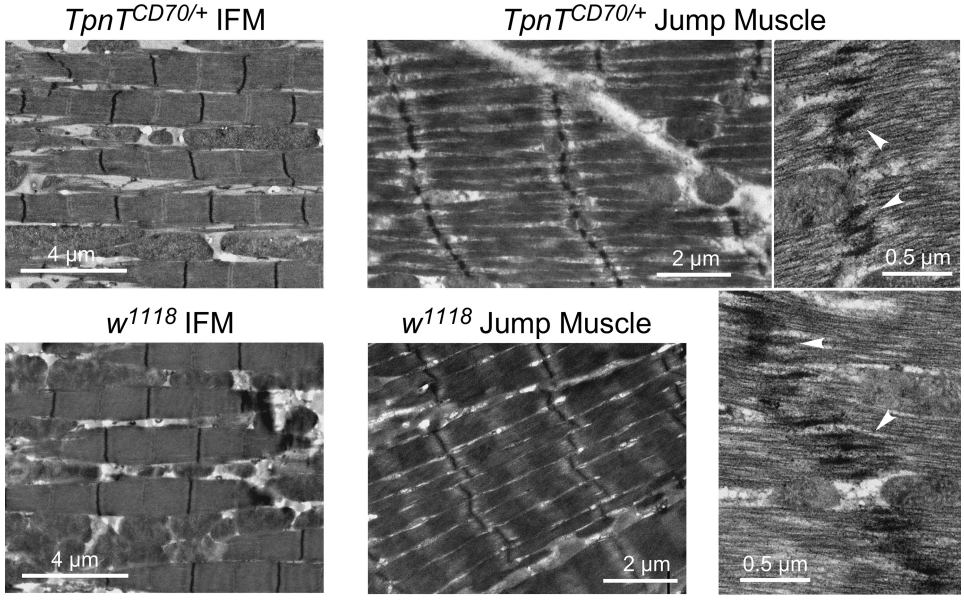

Figure 11. Transmission EM images of $TpnT^{CD70/+}$ fly muscles. IFM and jump muscle of 14-day-old $TpnT^{CD70/+}$ flies showed no significant destruction in sarcomere structures as compared with age-matched w^{1118} controls. However, the ultrastructural images detected signs of Z-band streaming in the $TpnT^{CD70/+}$ jump muscles (indicated with *white arrowheads* in the higher magnification *panels to the right*).

retains physiological binding to tropomyosin, TnI, and TnC (Fig. 4).

The ELISA protein binding test involves multiple high-stringency washes, and thus it reflects high-binding affinities of TpnT–CD70 protein for its three known physiological partners in the myofilaments. Although we did not have an intact *Drosophila* TnT protein as control due to the toxicity in bacterial expression, the binding affinities of TpnT–CD70 proteins to vertebrate tropomyosin, TnI, and TnC are comparable with that of chicken fast TnT, a native binding partner of vertebrate tropomyosin, TnI, and TnC used in the assay (Fig. 4), demonstrating preserved core functions of TpnT–CD70 proteins.

The preserved tropomyosin-, TnI-, and TnC-binding sites in TpnT–CD70 protein also support that the C-terminal extension of insect TnT is an evolutionarily-added structure similar to the N-terminal variable region of vertebrate TnT (9). Because the C-terminal extension is common among flying insects, it may serve an evolutionarily selected function with a fitness value in insect muscle specific to high-efficiency flight activities.

mAb 2C12 provides a common tool for Drosophila muscle and heart research

The 2C12 mAb that we developed in this study shows high affinity and specificity to *Drosophila* TnT in Western blotting and ELISA (Fig. 6). It is able to detect intact and CD70 truncated *Drosophila* TnT as well as spliced variants containing various combinations of alternative exons in the N-terminal variable region (exons 3–5) and the C-terminal region (exons 10A and 10B) (Fig. 6 and Fig. 7*A*). Therefore, mAb 2C12 must recognize an epitope encoded by constitutively-spliced exon(s) in the middle region of *Drosophila* TnT. The fact that mAb 2C12 does not recognize any vertebrate TnT (Fig. 6*A*) reflects a significantly diverged structure in *Drosophila* TnT, which is not directly involved in the binding sites for other myofilament proteins. The data show that mAb 2C12 provides a useful tool for the detection of *Drosophila* TnT in muscle and heart studies.

Identification of the two major N-terminal alternative splice forms expressed in adult fly muscles

In addition to identification and cloning of a novel splice form of *Drosophila* TnT from whole-body RNA extract (Fig. 2), we have cloned cDNAs that encode the major high- and low-molecular-weight TnT protein variants expressed in normal adult *Drosophila* muscles. By expressing the cloned cDNAs in *E. coli* for use as protein gel mobility controls, we identified the major splice form of TnT expressed in thoracic muscles (Fig. 7*A*) as the low-molecular-weight variant with exons 3–5 excluded (Fig. 2), consistent with a previous report (13). In jump muscles, two major splice forms of TnT are present (Fig. 7*B*), of which the low-molecular-weight variant is the same as the major form in thoracic muscles, whereas the high-molecular-weight variant has the alternative exons 3–5 all included (Fig. 2).

Expression of cDNAs encoding CD70-truncated *Drosophila* TnT with known N-terminal variations in bacterial culture provided control proteins for use as SDS gel mobility markers to identify C-terminal truncated TnT variants in the muscles of $TpnT^{CD70/+}$ mutant flies (Fig. 7). The results verified that the insertion of CD70 stop codon in exon 11 of the *TpnT* gene did not alter the native N-terminal alternative splicing pattern of *TpnT* RNA, further validating the $TpnT^{CD70/+}$ mutant fly for use in focused studies on the function of the C-terminal Glu-rich extension of TnT.

Embryonic lethality of $TpnT^{CD70}$ mutation

The embryonic lethal phenotype of $TpnT^{CD70}$ mutation causing 100% male lethality (Table 1) requires validation because the C-terminal extension–truncated TnT retains core functions (Fig. 4), effectively expresses in myocytes, and integrates into myofilaments (Fig. 7). The mutant flies were generated by CRISPR/Cas9 gene editing that may cause off-target mutations that could be X-linked and lethal. A more likely explanation is that the effect of deleting the Glu-rich C-terminal extension of *Drosophila* TnT on decreasing muscle contractility as seen in heterozygote female flies may be critical to the contractility of early embryonic muscles in generating sufficient force for successful hatching. Detailed developmental studies are merited to identify the primary mechanism for the embryonic lethality of $TpnT^{CD70}$ mutation.

Dominantly-negative phenotypes of TpnT–CD70 in muscle and heart

Decreased functions are observed in both flight and leg muscles, as well as in cardiac muscle of $TpnT^{CD70/+}$ flies, indicating the loss of a commonly important function. As no other muscle function-related genes are present near the *TpnT* locus, the significantly decreased muscle and heart functions of $TpnT^{CD70/+}$ flies are attributed to dominantly-negative effects of the mutation.

The phenotypes of $TpnT^{CD70/+}$ flies are distinct from that reported previously for splicing or single amino acid missense mutations such as upheld and indented thorax (11), muscleblind myotonic dystrophy (12), and abnormal muscle development (13). In contrast to the destruction of conserved core structure or a complete loss of function as reported in previous studies, the TpnT–CD70 mutant produces unique dominant effects on muscle and heart functions (Figs. 8 and 9*A*) with various proportions of the truncated protein (Fig. 7) to indicate a critical role of the Glu-rich C-terminal extension of *Drosophila* TnT.

Previous studies have documented an inverse correlation between baseline free Ca^{2+} and sarcomere length (24). Previous studies also established that decreased intracellular calcium weakens muscle contraction (25). An increase of sarcomere length in cardiac muscle at diastole is an adaptation to utilize the Frank-Starling mechanism for compensating weakened contractility (26), which is also a fundamental property of skeletal muscles (27). Although the overall development, growth, and structure of $TpnT^{CD70/+}$ fly muscles are apparently normal, the increased resting length of sarcomeres in jump muscle and heart but not in IFM (synchronous *versus* asynchronous muscles) (Fig. 10) may correspond to muscle weakness as well as indicate the lower intracellular Ca^{2+} suggested by the cardiac-pacing experiment (Fig. 9, *B* and *C*).

EM images detected the presence of Z-band streaming in $TpnT^{CD70/+}$ fly jump muscle (Fig. 11), which is often a sign of workload and/or muscle weakness–caused injury (28). This mechanical load and stretch-induced phenotype was not detected in IFM of the same flies. Therefore, the potentially synchronous muscle-specific impact of TpnT–CD70 is worth further investigation. To study the contractility of isolated muscle preparations from $TpnT^{CD70/+}$ flies should provide mechanistic insights into the physiological function of the Glu-rich C-terminal extension of insect TnT.

Potential role of the Glu-rich C-terminal extension of insect TnT as a myofilament Ca^{2+} reservoir

Although the overall cardiac function is decreased (Fig. 9*A*), consistent with the skeletal muscle phenotypes in Fig. 8, the hearts of $TpnT^{CD70/+}$ flies showed a significantly higher tolerance to Ca^{2+} overloading with less cardiac arrest/fibrillation during high frequency pacing (Fig. 9, *B* and *C*). This finding implicates a lower baseline Ca^{2+} content in the cardiomyocytes.

The insect muscle-specific Glu-rich C-terminal extension of TnT shows a striking similarity in amino acid sequence to the N-terminal variable region of avian pectoral muscle TnT (Fig. 1*C*). We previously found that the Glu-rich segment of avian pectoral muscle TnT has an intriguing capacity to bind Ca^{2+} with an affinity of ~14 μM, just below that of the regulatory Ca^{2+}-binding sites of TnC (19). It is interesting to note that this segment is absent in the TnT of the emu, a flightless bird (Fig. 1*B*). Therefore, this unique structure may function as a myofilament Ca^{2+} reservoir residing closely to TnC as a local Ca^{2+} buffer that might reduce the amount of Ca^{2+} to be cycled between cytoplasm and sarcoplasmic reticulum (and the extracellular compartment) during muscle contraction and relaxation. This mechanism would reduce the energy expenditure of Ca^{2+} pumps and increase the energetic efficiency of muscle, which is important for sustaining the highly-demanding muscle work during flight, especially the high-frequency and asynchronous contraction of insect IFM.

In this hypothesis, the deletion of the Glu-rich C-terminal 70 amino acids of *Drosophila* TnT removes a potential myofilament Ca^{2+} reservoir/buffer to decrease the level of free intracellular Ca^{2+} in resting myocytes. This effect may chronically lower the total calcium contents in the myocytes to decrease contractility (25), as shown by the overall muscle weakness in $TpnT^{CD70/+}$ flies. The loss of the Ca^{2+} reservoir function of TpnT–CD70 protein to reduce the total calcium content of myocyte is supported by the increased tolerance of the mutant fly heart to pacing-induced calcium overloading (Fig. 9, *B* and *C*).

This notion suggests a novel mechanism in calcium regulation of striated muscle contraction. Further studies by imaging Ca^{2+} dynamics in beating $TpnT^{CD70/+}$ fly hearts may validate this potentially underlying mechanism. To overcome the limitation that whole fly body electrical pacing is not cardiac muscle-specific, the use of an optogenetic reagent, channelrhodopsin-2, for heart-specific and noninvasive pacing as reported in a recent study (29) may be considered.

In conclusion, this study suggests that the Glu-rich segments independently evolved in TnT of insect and bird muscles may provide a novel mechanism to facilitate muscle contraction and relaxation as well as to reduce the energy expenditure for calcium cycling in these flying species. To further establish this function of TnT may lead to the development of a new treatment of muscle weaknesses and heart failure.

Experimental procedures

This research is approved by the Institutional Animal Care and Use Committee of Wayne State University.

Cloning of cDNAs encoding Drosophila TnT and construction of C-terminal deletion mutants

Total RNA was extracted from whole bodies of adult w^{1118} flies using the TRIzol reagent. Two μg of total RNA was used as template for reverse transcription (RT) of poly(A) mRNA using an anchored oligo(dT) primer (TV20). PCR amplification of cDNA corresponding to the entire coding region of *Drosophila TpnT* mRNA was performed using a pair of primers, one specific to the translation initiation codon site in exon 2, and the other specific to the translation termination codon site in exon 11. The amplified cDNA with expected size was digested at a 5′ NdeI site and a 3′ EcoRI site introduced by the PCR primers for insertion into NdeI- and EcoRI-cut pAED4 plasmid. Colonies of JM109 *E. coli* transformed with the recombinant plasmids were screened using PCR.

To identify cDNA clones containing the mutually-exclusive exon 10A or exon 10B, which cannot be distinguished by size, PCR using exon 10A- and exon 10B-specific primers was employed. A *Drosophila TpnT* cDNA encoding an N-terminal alternatively spliced low-molecular-weight variant expressed in flight muscles containing exon 10A in the C-terminal region was reconstructed by exchanging a restriction fragment from an exon 10B cDNA clone to generate a comparable pair of exon 10A/10B variants. cDNAs encoding C-terminal 70 amino acid–truncated *Drosophila* TnT (TpnT–CD70) were then constructed using PCR with a mutagenesis reverse primer to introduce a premature stop codon. All cloned *Drosophila* TpnT cDNAs and mutants were confirmed by DNA sequencing.

Expression of Drosophila TpnT–CD70 in E. coli and purification

C-terminal truncated *Drosophila* TpnT–CD70 – exon 10A and TpnT–CD70 – exon 10B proteins were expressed in transformed BL21(DE3)pLysS *E. coli* cultured in 2× TY media containing 100 mg/liter ampicillin and 25 mg/liter chloramphenicol. After induction with 0.4 mM isopropyl β-D-1-thiogalactopyranoside at mid-log phase in a 37 °C shaking incubator for 3 h, the bacterial cells were harvested by centrifugation.

The purification steps were carried out at 4 °C. The cell pellets were resuspended in lysis buffer (50 mM sodium phosphate buffer, pH 8.0, 2 mM EDTA, 1 mM PMSF, 15 mM β-mercaptoethanol) and lysed using a French cell press. The bacterial lysate was centrifuged to remove any insoluble materials and fractionated by ammonium sulfate precipitation. The 30–50% saturation fraction enriched with TpnT–CD70 protein was dialyzed against deionized water, added solid urea to 6 M, EDTA to 0.1 mM, β-mercaptoethanol to 6 mM, PMSF to 0.5 mM, adjusted to pH 5.6 with 20 mM sodium acetate buffer, and centrifuged to remove any precipitates before loading on a CM52 cation–exchange column equilibrated in 6 M urea, 20 mM sodium acetate, pH 5.6. The column was eluted with a linear gradient of 0–500 mM KCl, and the $A_{280\,nm}$ peaks were analyzed by SDS-PAGE to identify the fractions containing TpnT–CD70 protein. The TpnT–CD70 fractions were pooled, dialyzed against 0.1 mM EDTA, and lyophilized.

Development of a specific mAb against Drosophila TnT

To develop an anti-*Drosophila* TnT monoclonal antibody (mAb) for use as a detection tool, a short-term immunization procedure was used to immunize a 5-week-old female BALB/c mouse. As described previously (30), the initial immunization was done by intraperitoneal and intramuscular injections of a total of 100 μg of purified TpnT–CD70 protein (1:1 mix of the exon 10A and exon 10B variants) in 100 μl of PBS mixed with an equal amount of Freud's complete adjuvant. On day 11 and 12 after the primary immunization, the mouse was boosted intraperitoneally with 100 μg of TpnT–CD70 protein in 150 μl of PBS without adjuvant. On day 14, the mouse was euthanized, and spleen cells were harvested to fuse with SP2/mIL-6 mouse myeloma cells (ATCC CRL-2016) using 50% polyethylene glycol 3500 containing 7% DMSO. Hybridoma colonies were selected with HAT (0.1 mM hypoxanthine, 0.4 μM aminopterin, and 16 μM thymidine) media containing 20% fetal bovine serum and screened using indirect enzyme-linked immunosorbent assay (ELISA) against purified TpnT–CD70 protein using horseradish peroxidase (HRP)-conjugated anti-mouse immunoglobulin secondary antibody (Santa Cruz Biotechnology). Positive hybridoma clones secreting anti-TpnT mAb were subcloned three or four times using the limiting dilution method. Multiple vials of the final generation of positive hybridoma subclones were stored in liquid nitrogen. Exhausted hybridoma cell culture supernatant of mAb 2C12 was collected for characterization and lyophilized in aliquots for uses in the detection of *Drosophila* TnT.

SDS-PAGE and Western blotting

Protein samples were prepared in SDS-PAGE sample buffer, heated at 80 °C for 5 min, and clarified by centrifugation. The samples were electrophoresed in 14% SDS-polyacrylamide gel with an acrylamide/bisacrylamide ratio of 180:1, as described previously (31). The resulting gels were stained with Coomassie Blue R-250 and de-stained in 10% acetic acid to visualize the protein bands.

Duplicated SDS-polyacrylamide gels were blotted on nitrocellulose membrane using a semi-dry electron transfer apparatus from Bio-Rad. The blotted membranes were blocked with 1% bovine serum albumin (BSA) in Tris-buffered saline (TBS, 136.9 mM NaCl, 2.7 mM KCl, 25 mM Tris-HCl, pH 7.4) at room temperature for 45 min and incubated with anti-TpnT mAb 2C12 diluted in TBS containing 0.1% BSA at room temperature for 2 h. Following washes with TBS containing 0.5% Triton X-100 and 0.05% SDS, the membranes were incubated with alkaline phosphatase-labeled anti-mouse IgG secondary antibody (Santa Cruz Biotechnology), washed as above, and developed in 5-bromo-4-chloro-3-indolyl phosphate and nitro blue tetrazolium substrate solution, as described previously (32).

Microtiter plate ELISA protein–binding assay

ELISA solid-phase protein–binding experiments were performed to assess the binding of C-terminal truncated *Drosophila* TnT with TnI, TnC, and tropomyosin. As described previously (33), purified TpnT–CD70 exon 10A, TpnT–CD70 exon 10B, and chicken fast TnT control (17) proteins were coated on 96-well microtiter plates at 2 μg/ml in Buffer A (0.1 M KCl, 3 mM $MgCl_2$, 10 mM PIPES, pH 7.0), 100 μl/well at 4 °C overnight. The plates were washed with Buffer T (0.05% Tween 20 in Buffer A) and blocked with Buffer B (Buffer T plus 1% BSA) at room temperature for 1 h. Serial dilutions of tissue-purified bovine cardiac TnI, rabbit α-tropomyosin, and recombinant mouse fast TnC were added to triplicate wells in Buffer D (Buffer T plus 0.1% BSA) to incubate at room temperature for 2 h. The TnC-binding assay was done in the presence of 0.1 mM $CaCl_2$ or 0.1 mM EGTA.

The core function of TpnT–CD70 in binding these conserved myofilament proteins was examined via anti-TnI mAb TnI-1 (34), anti-α-tropomyosin mAb CH1 (23), and anti-fast TnC mAb 2C3 (35), respectively, diluted in Buffer D. After incubation with the primary antibodies at room temperature for 1 h and washes with Buffer T, HRP-conjugated anti-mouse immunoglobulin secondary antibody was added to the plates and incubated at room temperature for 45 min. After final washes with Buffer T, H_2O_2/2,2′-azino-bis(3-ethylbenzthiazoline sulfonic acid) substrate was added for color development at room temperature. Absorbance at 420 nm was read using an automated microplate reader at 5-min intervals for 30 min. Protein-binding curves were derived from data collected at a time point prior to the end of the linear phase of color development.

Generation and maintenance of TpnT–CD70 flies

Drosophila TpnT–CD70 mutation was constructed in the w^{1118} strain with CRISPR/Cas9 gene editing at a commercial service facility (Well Genetics, Taiwan, Republic of China). To express the C-terminal 70-amino acid–deleted TnT, a stop codon was inserted into the exon 11 sequence of *TpnT* gene. An RFP selection marker cassette was introduced after the stop codon, which was removed with Cre-loxP recombination after successful establishment of the mutant fly line. The mutant *TpnT–CD70* allele was identified using PCR, and both RFP^+ and RFP^- lines were separately maintained as heterozygotes in a stable line balanced with FM7a (*TpnT–CD70/FM7a*, referred to as $TpnT^{CD70/+}$ in this study).

The flies were maintained at 25 °C and 50% humidity on a 12-h light/dark cycle with a standard 10% sucrose and 10% yeast diet. Flies were housed at constant density for at least two generations prior to phenotype studies. Gravid female $TpnT^{CD70/+}$ or w^{1118} flies were bred in aerated 6-oz bottles capped with grape juice agar plates spread with a small amount of yeast paste (36) for 48 h, at which time the adults were removed, and total embryos were counted. Embryos were transferred to 6-oz bottles containing standard 10% sucrose, 10% yeast media and allowed to develop at 25 °C. Viable adults were phenotypically scored and counted. Experiments were performed in at least duplicate.

The expression of TpnT–CD70 protein in *Drosophila* muscles was examined using Western blotting. Indirect flight muscle and jump muscle were isolated from adult flies anesthetized with Flynap (triethylamine), as described previously (37). SDS-PAGE of total muscle protein extract and Western blotting using mAb 2C12 were done as above. Muscles of age-matched w^{1118} flies and total protein extracted from w^{1118} larvae were used as controls.

Examination of Drosophila muscle functions in vivo

Functional studies were performed in 5- and 14-day-old flies, as described previously (38–41). All assays were performed in triplicate with age-matched $TpnT^{CD70/+}$ and w^{1118} (Well Genetics) background controls.

Acute flight ability was assessed by gravity dropping 160 flies per genotype into a cylindrical acrylic tube containing a polycarbonate sheet coated with Tangle-Trap glue. The sheet was removed, placed against a white background, and photographed. Landing height of the flies was assessed using ImageJ software (National Institutes of Health, Bethesda, MD).

Climbing velocity was assessed by measuring the distance that flies climbed in 2 s. Five vials of 20 flies each were secured in a vial rack and placed in front of a white background. The vial rack was manually lifted and dropped to knock the flies to the bottom of the vial. The flies' progress was photographed 2 s after the drop, with four repetitions. The four pictures were analyzed using ImageJ software. The height of the vials was divided into four quadrants, and the total number of flies in each quadrant were used to generate a climbing index as described (39, 40).

To assess fatigue tolerance, climbing endurance was measured as described (39). Eight vials containing 20 flies each per experimental group were placed on a negative geotaxis machine (Power Tower), which induces flies to repetitively climb vials until fatigue. A vial of flies was scored as fatigued when 80% of the flies in the vial stopped initiating the climbing response for three consecutive stimuli.

Cardiac pacing

External electrical cardiac pacing was performed as described previously (41). Using a modified microscope slide, wire leads were connected to a square-wave electric stimulator that allowed experimental control of heart rate in anesthetized live flies.

To test cardiac stress resistance, flies were paced at 40 volts and 6 Hz for 30 s. Immediately after pacing, fly hearts were visually scored through the transparent abdominal cuticle for either arrest or fibrillation. The percentage of flies that experienced either arrest or fibrillation was reported as the failure rate.

To assess the response of fly cardiomyocytes to acute Ca^{2+} overloading, a high-frequency cardiac-pacing protocol was developed. Anesthetized flies were placed on the pacing apparatus as above and paced at progressively increasing frequencies at constant voltage (40 V) for 5-s episodes with 5-s rest intervals. Flies were paced until hearts exhibited initial failure after a pacing episode. Cardiac fibrillation and arrest were scored and plotted separately as mortality curves.

Fluorescence confocal microscopy

Heart and thoracic muscle from 14-day-old *kettin GFP* (control, DGRC stock no. 110855 (42)) or $TnT^{CD70/+}$*;;kettin GFP* flies were fixed and stained using the protocols described previously (43, 44) with the following modifications. Adult control and experimental flies were rapidly dissected ventral side up in relaxing solution (RS) containing 20 mM sodium phosphate buffer, pH 7.0, 5 mM $MgCl_2$, and 5 mM EGTA. Flies were prefixed in RS plus 4% formaldehyde (FA) for 30 min and washed with relaxing buffer, and thoraces and abdomens were separated into wells of a 96-well plate for a second 15-min incubation in RS and a final 15-min RS + FA fixation. Hearts and thoraces were separately blocked in PBS, 0.05% Tween 20 (PBS-T) plus 10% normal goat serum (NGS) and stained with chicken anti-GFP antibody (Invitrogen) in PBS-T plus 10% NGS and goat anti-chicken and goat anti-mouse secondary antibodies. Alexa fluor 488 goat anti-chicken secondary antibody (Invitrogen) was applied in the same buffer supplemented with Alexa fluor 594-Phalloidin (Invitrogen) to co-stain F-actin.

Imaging was performed using a Leica DMI 6000 scope outfitted with a Photometrics Prime 95B CMOS camera and X-light spinning disc. Images were taken using ×40 dry and ×100 oil immersion lens, and sarcomere length measurement was performed on the ×100 lens images using ImageJ software. Ten images were acquired for each sample, and experiments were performed in duplicate.

Transmission EM

14-Day-old $TpnT^{CD70/+}$ and w^{1118} flies were euthanized using Flynap and fixed in 1% paraformaldehyde and 1% EM grade glutaraldehyde in PBS. The specimens were sent for transmission electron microscopic imaging of muscle ultrastructure at the Central Microscopy Research Facility at the University of Iowa.

Data analysis

SDS gels and Western blots were scanned at 600 p.s.i. for data documentation and densitometry quantification. Statistical analyses were done using paired Student's *t* test for mAb affinity, protein binding, and stoichiometry analysis, one-way analysis of variance for fly muscle functional studies, χ^2 test for chronic cardiac pacing, and a log-rank test for fatigue resistance and high-frequency cardiac pacing studies.

Author contributions—T. Cao, A. S., and T. Cobb data curation; T. Cao, A. S., and T. Cobb formal analysis; T. Cao, A. S., T. Cobb, R. J. W., and J.-P. J. validation; T. Cao, A. S., R. J. W., and J.-P. J. investigation; T. Cao, T. Cobb, and A. S. visualization; T. Cao, A. S., R. J. W., and J.-P. J. methodology; T. Cao, A. S., T. Cobb, R. J. W., and J.-P. J. writing-original draft; T. Cao, A. S., R. J. W., and J.-P. J. writing-review and editing; R. J. W. and J.-P. J. resources; R. J. W. and J.-P. J. funding acquisition; J.-P. J. conceptualization; J.-P. J. supervision; J.-P. J. project administration.

Acknowledgment—We thank Dr. Han-Zhong Feng for providing the vertebrate muscle SDS-PAGE samples and assistance in the isolation of fly muscles.

References

1. Rassier, D. E. (2017) Sarcomere mechanics in striated muscles: from molecules to sarcomeres to cells. *Am. J. Physiol. Cell Physiol.* **313,** C134–C145 CrossRef Medline
2. Yanagida, T., Arata, T., and Oosawa, F. (1985) Sliding distance of actin filament induced by a myosin crossbridge during one Atp hydrolysis cycle. *Nature* **316,** 366–369 CrossRef Medline
3. Gordon, A. M., Homsher, E., and Regnier, M. (2000) Regulation of contraction in striated muscle. *Physiol. Rev.* **80,** 853–924 CrossRef Medline

4. Sanger, J. W., Wang, J., Fan, Y., White, J., Mi-Mi, L., Dube, D. K., Sanger, J. M., and Pruyne, D. (2017) Assembly and maintenance of myofibrils in striated muscle. *Handb Exp Pharmacol.* **235,** 39–75 CrossRef Medline
5. Jin, J. P., Zhang, Z., and Bautista, J. A. (2008) Isoform diversity, regulation, and functional adaptation of troponin and calponin. *Crit. Rev. Eukaryot. Gene Expr.* **18,** 93–124 CrossRef Medline
6. Cao, T., Thongam, U., and Jin, J. P. (2019) Invertebrate troponin: insights into the evolution and regulation of striated muscle contraction. *Arch. Biochem. Biophys.* **666,** 40–45 CrossRef Medline
7. Kagawa, H., Takaya, T., Ruksana, R., Anokye-Danso, F., Amin, M. Z., and Terami, H. (2007) *C. elegans* model for studying tropomyosin and troponin regulations of muscle contraction and animal behavior. *Adv. Exp. Med. Biol.* **592,** 153–161 CrossRef Medline
8. Tobacman, L. S. (1996) Thin filament-mediated regulation of cardiac contraction. *Annu. Rev. Physiol.* **58,** 447–481 CrossRef Medline
9. Chong, S. M., and Jin, J. P. (2009) To investigate protein evolution by detecting suppressed epitope structures. *J. Mol. Evol.* **68,** 448–460 CrossRef Medline
10. Bullard, B., and Pastore, A. (2011) Regulating the contraction of insect flight muscle. *J. Muscle Res. Cell Motil.* **32,** 303–313 CrossRef Medline
11. Fyrberg, E., Fyrberg, C. C., Beall, C., and Saville, D. L. (1990) *Drosophila melanogaster* troponin-T mutations engender three distinct syndromes of myofibrillar abnormalities. *J. Mol. Biol.* **216,** 657–675 CrossRef Medline
12. Vicente-Crespo, M., Pascual, M., Fernandez-Costa, J. M., Garcia-Lopez, A., Monferrer, L., Miranda, M. E., Zhou, L., and Artero, R. D. (2008) *Drosophila* muscleblind is involved in troponin T alternative splicing and apoptosis. *PLoS ONE* **3,** e1613 CrossRef Medline
13. Nongthomba, U., Ansari, M., Thimmaiya, D., Stark, M., and Sparrow, J. (2007) Aberrant splicing of an alternative exon in the *Drosophila* troponin-T gene affects flight muscle development. *Genetics* **177,** 295–306 CrossRef Medline
14. Domingo, A., González-Jurado, J., Maroto, M., Díaz, C., Vinós, J., Carrasco, C., Cervera, M., and Marco, R. (1998) Troponin-T is a calcium-binding protein in insect muscle: in vivo phosphorylation, muscle-specific isoforms and developmental profile in *Drosophila melanogaster*. *J. Muscle Res. Cell Motil.* **19,** 393–403 CrossRef Medline
15. Jin, J. P., Chen, A., and Huang, Q. Q. (1998) Three alternatively spliced mouse slow skeletal muscle troponin T isoforms: conserved primary structure and regulated expression during postnatal development. *Gene* **214,** 121–129 CrossRef Medline
16. Wang, J., and Jin, J. P. (1997) Primary structure and developmental acidic to basic transition of 13 alternatively spliced mouse fast skeletal muscle troponin T isoforms. *Gene* **193,** 105–114 CrossRef Medline
17. Ogut, O., Granzier, H., and Jin, J. P. (1999) Acidic and basic troponin T isoforms in mature fast-twitch skeletal muscle and effect on contractility. *Am. J. Physiol.* **276,** C1162–C1170 CrossRef Medline
18. Jin, J. P., and Samanez, R. A. (2001) Evolution of a metal-binding cluster in the NH_2-terminal variable region of avian fast skeletal muscle troponin T: functional divergence on the basis of tolerance to structural drifting. *J. Mol. Evol.* **52,** 103–116 CrossRef Medline
19. Zhang, Z., Jin, J. P., and Root, D. D. (2004) Binding of calcium ions to an avian flight muscle troponin T. *Biochemistry* **43,** 2645–2655 CrossRef Medline
20. Wang, Z. Y., Sarkar, S., Gergely, J., and Tao, T. (1990) Ca^{2+}-dependent interactions between the C-helix of troponin-C and troponin-I. Photocross-linking and fluorescence studies using a recombinant troponin-C. *J. Biol. Chem.* **265,** 4953–4957 Medline
21. Feng, H. Z., Hossain, M. M., Huang, X. P., and Jin, J. P. (2009) Myofilament incorporation determines the stoichiometry of troponin I in transgenic expression and the rescue of a null mutation. *Arch. Biochem. Biophys.* **487,** 36–41 CrossRef Medline
22. Wang, X., Huang, Q. Q., Breckenridge, M. T., Chen, A., Crawford, T. O., Morton, D. H., and Jin, J. P. (2005) Cellular fate of truncated slow skeletal muscle troponin T produced by Glu^{180} nonsense mutation in Amish nemaline myopathy. *J. Biol. Chem.* **280,** 13241–13249 CrossRef Medline
23. Jin, J. P., and Chong, S. M. (2010) Localization of the two tropomyosin-binding sites of troponin T. *Arch. Biochem. Biophys.* **500,** 144–150 CrossRef Medline
24. Robinson, P., Liu, X., Sparrow, A., Patel, S., Zhang, Y. H., Casadei, B., Watkins, H., and Redwood, C. (2018) Hypertrophic cardiomyopathy mutations increase myofilament Ca^{2+} buffering, alter intracellular Ca^{2+} handling, and stimulate Ca^{2+}-dependent signaling. *J. Biol. Chem.* **293,** 10487–10499 CrossRef Medline
25. Shattock, M. J., Ottolia, M., Bers, D. M., Blaustein, M. P., Boguslavskyi, A., Bossuyt, J., Bridge, J. H., Chen-Izu, Y., Clancy, C. E., Edwards, A., Goldhaber, J., Kaplan, J., Lingrel, J. B., Pavlovic, D., Philipson, K., *et al.* (2015) Na^+/Ca^{2+} exchange and Na^+/K^+-ATPase in the heart. *J. Physiol.* **593,** 1361–1382 CrossRef Medline
26. van der Velden, J., de Jong, J. W., Owen, V. J., Burton, P. B., and Stienen, G. J. (2000) Effect of protein kinase A on calcium sensitivity of force and its sarcomere length dependence in human cardiomyocytes. *Cardiovasc. Res.* **46,** 487–495 CrossRef Medline
27. Hanft, L. M., and McDonald, K. S. (2010) Length dependence of force generation exhibit similarities between rat cardiac myocytes and skeletal muscle fibres. *J. Physiol.* **588,** 2891–2903 CrossRef Medline
28. Fridén, J., and Lieber, R. L. (1992) Structural and mechanical basis of exercise-induced muscle injury. *Med. Sci. Sports Exerc.* **24,** 521–530 Medline
29. Alex, A., Li, A., Tanzi, R. E., and Zhou, C. (2015) Optogenetic pacing in *Drosophila melanogaster*. *Sci. Adv.* **1,** e1500639 CrossRef Medline
30. Liu, R., Hossain, M. M., Chen, X., and Jin, J. P. (2017) Mechanoregulation of SM22α/transgelin. *Biochemistry* **56,** 5526–5538 CrossRef Medline
31. Jin, J. P. (1995) Cloned rat cardiac titin class I and class II motifs. Expression, purification, characterization, and interaction with F-actin. *J. Biol. Chem.* **270,** 6908–6916 Medline
32. Wang, J., and Jin, J. P. (1998) Conformational modulation of troponin T by configuration of the NH_2-terminal variable region and functional effects. *Biochemistry* **37,** 14519–14528 CrossRef Medline
33. Biesiadecki, B. J., and Jin, J. P. (2011) A high-throughput solid-phase microplate protein-binding assay to investigate interactions between myofilament proteins. *J. Biomed. Biotechnol.* **2011,** 421701 CrossRef Medline
34. Jin, J. P., Yang, F. W., Yu, Z. B., Ruse, C. I., Bond, M., and Chen, A. (2001) The highly conserved COOH terminus of troponin I forms a Ca^{2+}-modulated allosteric domain in the troponin complex. *Biochemistry* **40,** 2623–2631 CrossRef Medline
35. Jin, J. P., Chong, S. M., and Hossain, M. M. (2007) Microtiter plate monoclonal antibody epitope analysis of Ca^{2+}- and Mg^{2+}-induced conformational changes in troponin C. *Arch. Biochem. Biophys.* **466,** 1–7 CrossRef Medline
36. Rothwell, W. F., and Sullivan, W. (2007) Drosophila embryo collection. *CSH Protoc.* **2007,** pdb.prot4825 CrossRef
37. Chakraborty, K., VijayRaghavan, K., and Gunage, R. (2018) A method to injure, dissect and image indirect flight muscle of *Drosophila*. *Bio-Protocol.* **8,** CrossRef
38. Babcock, D. T., and Ganetzky, B. (2014) An improved method for accurate and rapid measurement of flight performance in *Drosophila*. *J. Vis. Exp. 2014,* **84,** e51223 CrossRef Medline
39. Damschroder, D., Cobb, T., Sujkowski, A., and Wessells, R. (2018) *Drosophila* endurance training and assessment of its effects on systemic adaptations. *Bio-Protocol.* **8,** CrossRef
40. Gargano, J. W., Martin, I., Bhandari, P., and Grotewiel, M. S. (2005) Rapid iterative negative geotaxis (RING): a new method for assessing age-related locomotor decline in *Drosophila*. *Exp. Gerontol.* **40,** 386–395 CrossRef Medline
41. Wessells, R. J., and Bodmer, R. (2004) Screening assays for heart function mutants in *Drosophila*. *BioTechniques* **37,** 58–60, 62, 64 passim CrossRef Medline
42. Morin, X., Daneman, R., Zavortink, M., and Chia, W. (2001) A protein trap strategy to detect GFP-tagged proteins expressed from their endogenous loci in *Drosophila*. *Proc. Natl. Acad. Sci. U.S.A.* **98,** 15050–15055 CrossRef Medline
43. Alayari, N. N., Vogler, G., Taghli-Lamallem, O., Ocorr, K., Bodmer, R., and Cammarato, A. (2009) Fluorescent labeling of *Drosophila* heart structures. *J. Vis. Exp.* **2009,** 1423 CrossRef Medline
44. Xiao, Y. S., Schock, F., and Gonzalez-Morales, N. (2017) Rapid IFM dissection for visualizing fluorescently tagged sarcomeric proteins. *Bio Protoc.* **7,** e2606 CrossRef Medline